

SUPPORTING INFORMATION

Tuning the coordination sphere of octahedral Dy(III) complexes with silanolate/stannanolate ligands: synthesis, structures and field-induced slow relaxation of the magnetization

Jérôme Long^{a,*}, Aleksei O. Tolpygin,^{c,d} Anton V. Cherkasov,^c Yulia V. Nelyubina,^d Yannick Guari,^a Joulia Larionova^a and Alexander A. Trifonov^{*c,d}

^a ICGM, Univ. Montpellier, CNRS, ENSCM, Montpellier, France. E-mail:
jerome.long@umontpellier.fr

^b Institut Universitaire de France (IUF), 1 rue Descartes, 75231 Paris Cedex 05, France.

^c Institute of Organometallic Chemistry of Russian Academy of Sciences, 49 Tropinina str.,
GSP-445, 603950, Nizhny Novgorod, Russia. E-mail: *trif@iomc.ras.ru*

^d A.N. Nesmeyanov Institute of Organoelement Compounds of Russian Academy of Sciences,
28 Vavilova str., 119334, Moscow, Russia.

TABLE OF CONTENTS

Figure S1: Perspective view of the crystal packing for 1 and 2 along the <i>b</i> crystallographic axes. Hydrogen atoms have been omitted for clarity.....	3
Figure S2: Perspective view of the crystal packing for 3 and 4 along the <i>b</i> crystallographic axes. Hydrogen atoms have been omitted for clarity.....	4
Figure S3: Temperature dependence of χT under an applied magnetic field of 1000 Oe for 1-4 Inset: field dependence of the magnetization at 1.8 K for 1-4.	5
Figure S4: Frequency dependence of χ' and χ'' for 1-4 for different temperatures performed in zero magnetic static field.	6
Figure S5: Cole-Cole (Argand) plots obtained using the ac susceptibility data for 4 in zero magnetic field. The solid lines correspond to the best fit obtained with a generalized Debye model	7
Figure S6: Frequency dependence of χ' and χ'' for 1-4 for various dc fields.	8
Figure S7: Field dependence of the relaxation time at 2 K (1-3) and 5 K (4). The solid line represents the fit with Eq. 2.	9
Figure S8: Frequency dependence of χ' and χ'' for different temperatures performed under a 500 (1-3) or 1000 (4) Oe dc field.	10
Figure S9: Cole-Cole (Argand) plots obtained using the ac susceptibility data for 1-3 (500 Oe) and 4 (1000 Oe). The solid lines correspond to the best fit obtained with a generalized Debye model.	11
Figure S10: Anisotropic axes (purple) obtained from the MAGELLAN package. ¹	12
 Table S1: Crystal data, data collection and structure refinement details for 1, 2, 3, 4.	13
Table S2: SHAPE analysis for 1-4.....	14
Table S3: Selected bond lengths (Å) and angles (deg) for 1-4.	15
Table S4: Fitting of the Cole-Cole plots with a generalized Debye model under a 0 Oe dc field for 4.	16
Table S5: Fit parameters of the field dependence of the relaxation time at 30 K for 1, 2 and 4.	16
Table S6: Fitting of the Cole-Cole plots with a generalized Debye model under a 500 Oe dc field for 1.	16
Table S7: Fitting of the Cole-Cole lots with a generalized Debye model under a 500 Oe dc field for 2.	17
Table S8: Fitting of the Cole-Cole plots with a generalized Debye model under a 500 Oe dc field for 3.	17
Table S9: Fitting of the Cole-Cole plots with a generalized Debye model under a 1000 Oe dc field for 4.	18

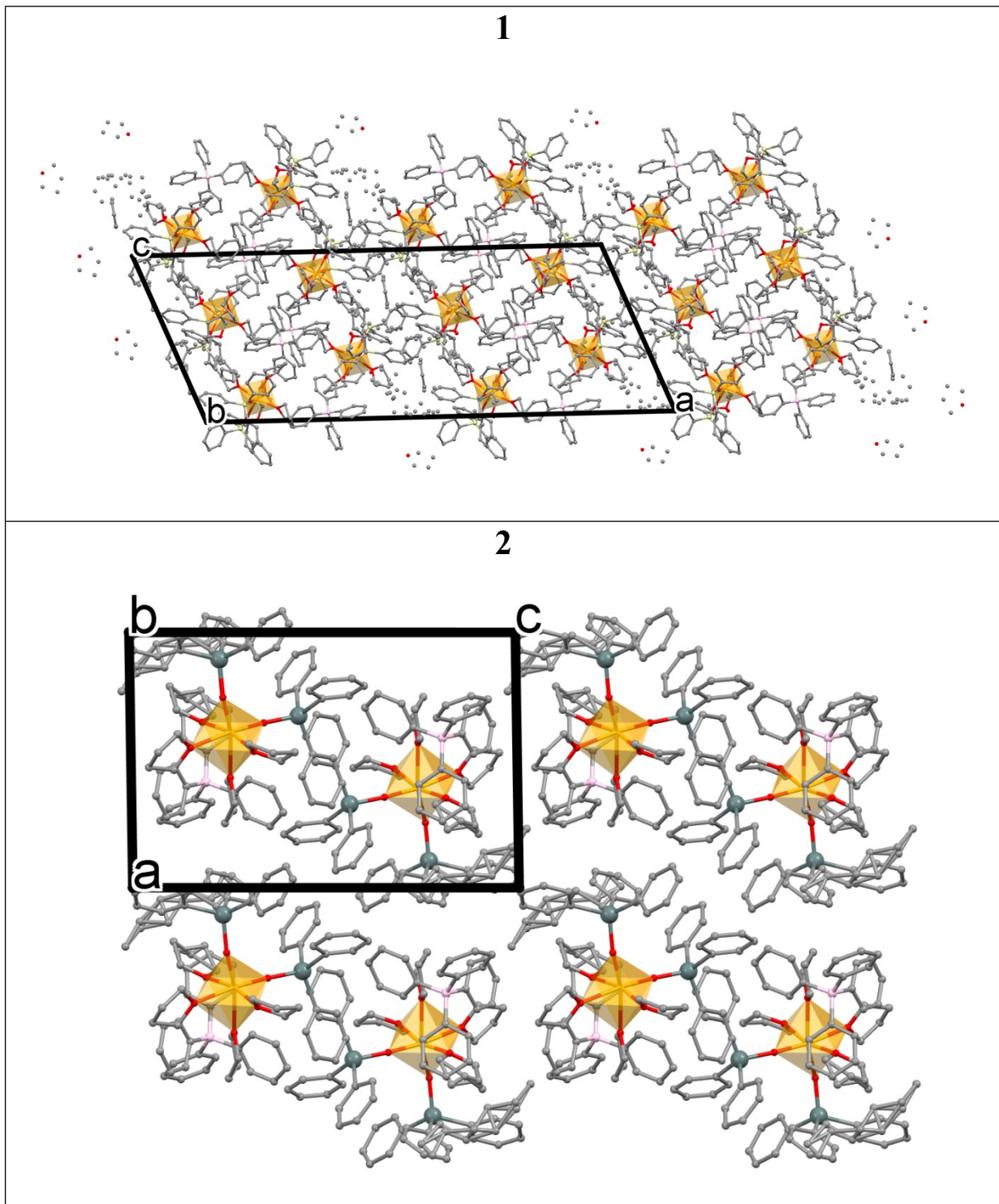
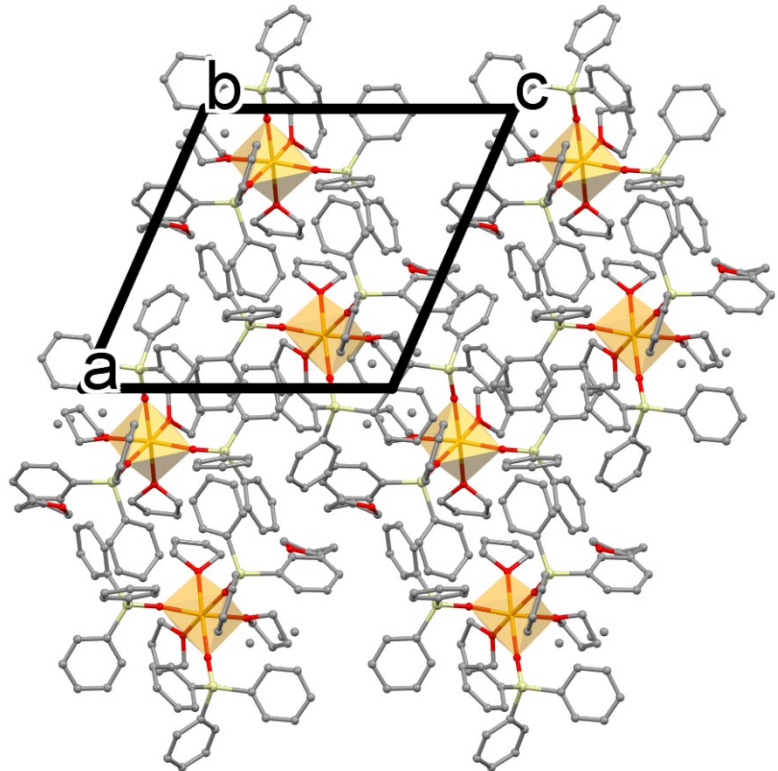


Figure S1: Perspective view of the crystal packing for **1** and **2** along the *b* crystallographic axes.

Hydrogen atoms have been omitted for clarity.

3



4

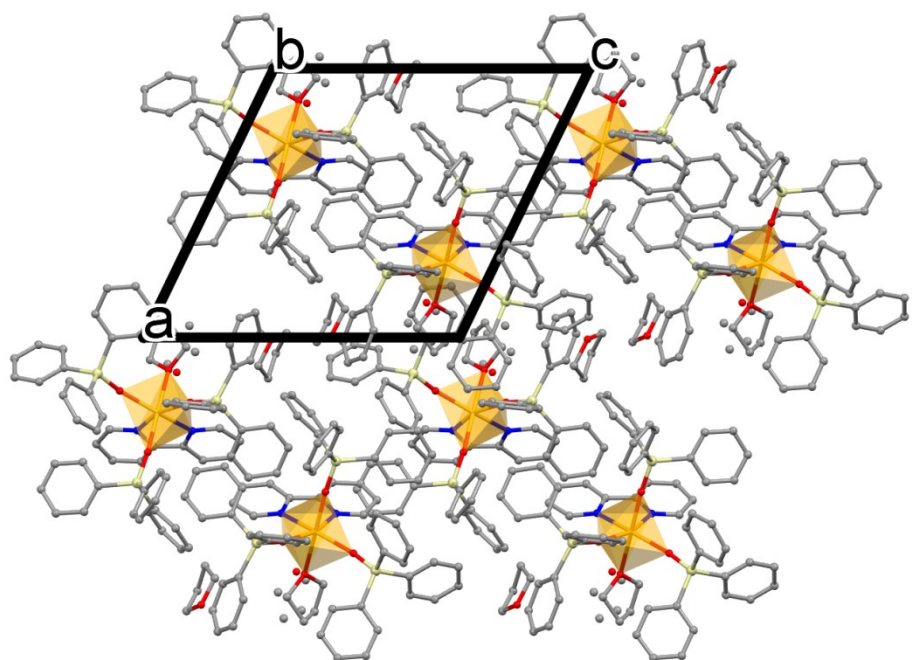


Figure S2: Perspective view of the crystal packing for **3** and **4** along the *b* crystallographic axes.

Hydrogen atoms have been omitted for clarity

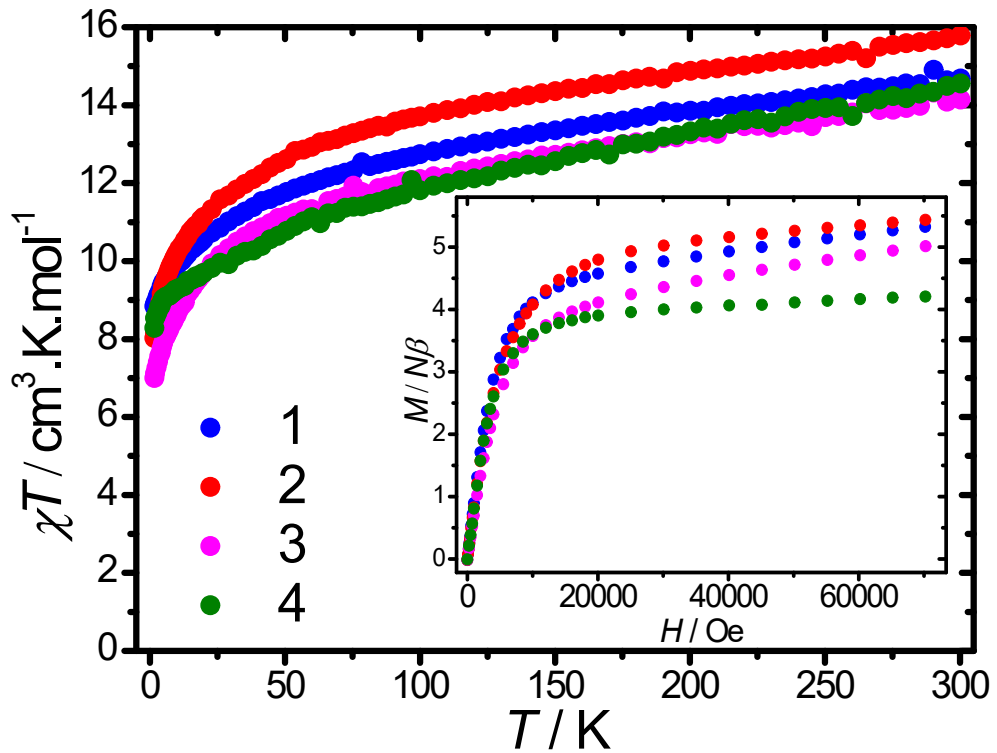


Figure S3: Temperature dependence of χT under an applied magnetic field of 1000 Oe for **1-4** Inset: field dependence of the magnetization at 1.8 K for **1-4**.

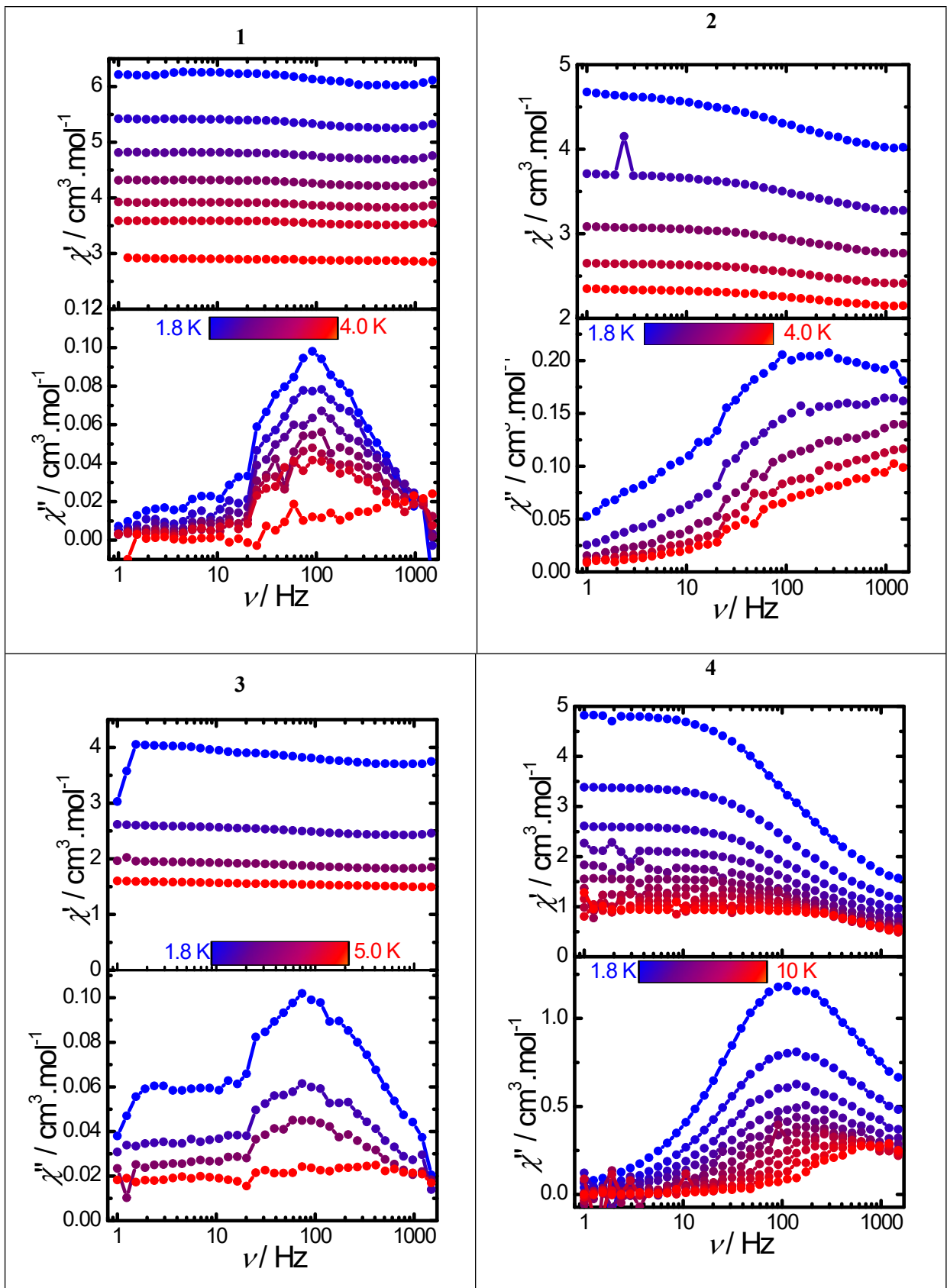


Figure S4: Frequency dependence of χ' and χ'' for 1–4 for different temperatures performed in zero magnetic static field.

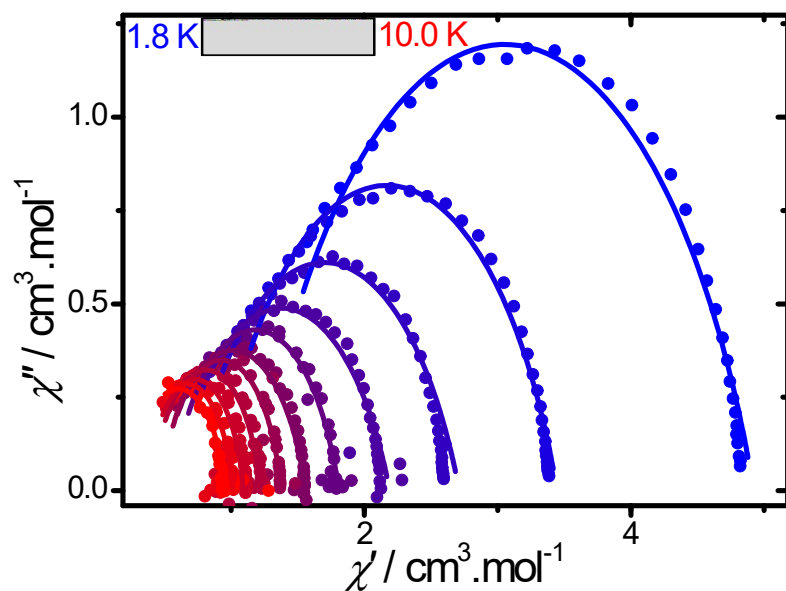


Figure S5: Cole-Cole (Argand) plots obtained using the ac susceptibility data for **4** in zero magnetic field. The solid lines correspond to the best fit obtained with a generalized Debye model

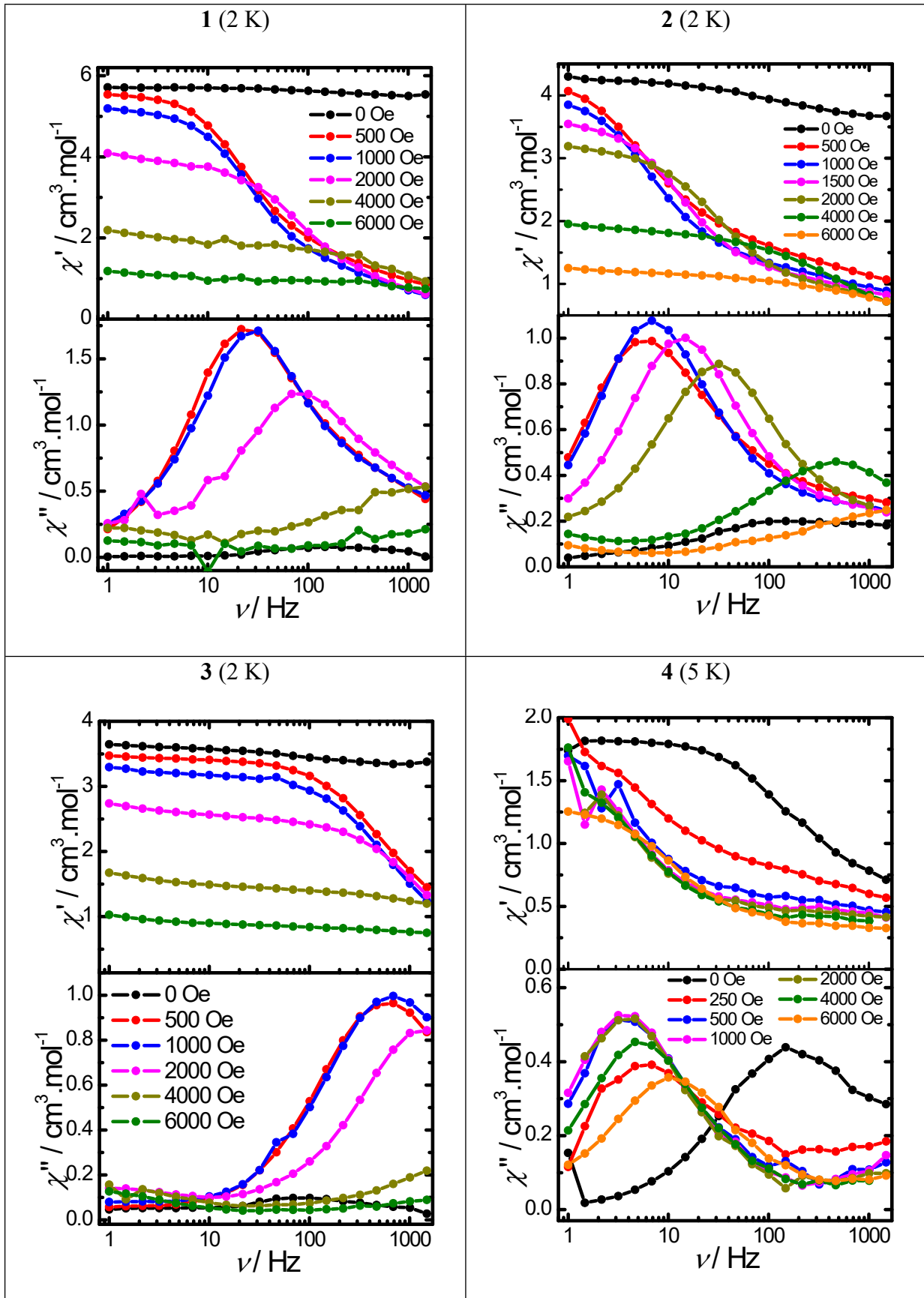


Figure S6: Frequency dependence of χ' and χ'' for 1-4 for various dc fields.

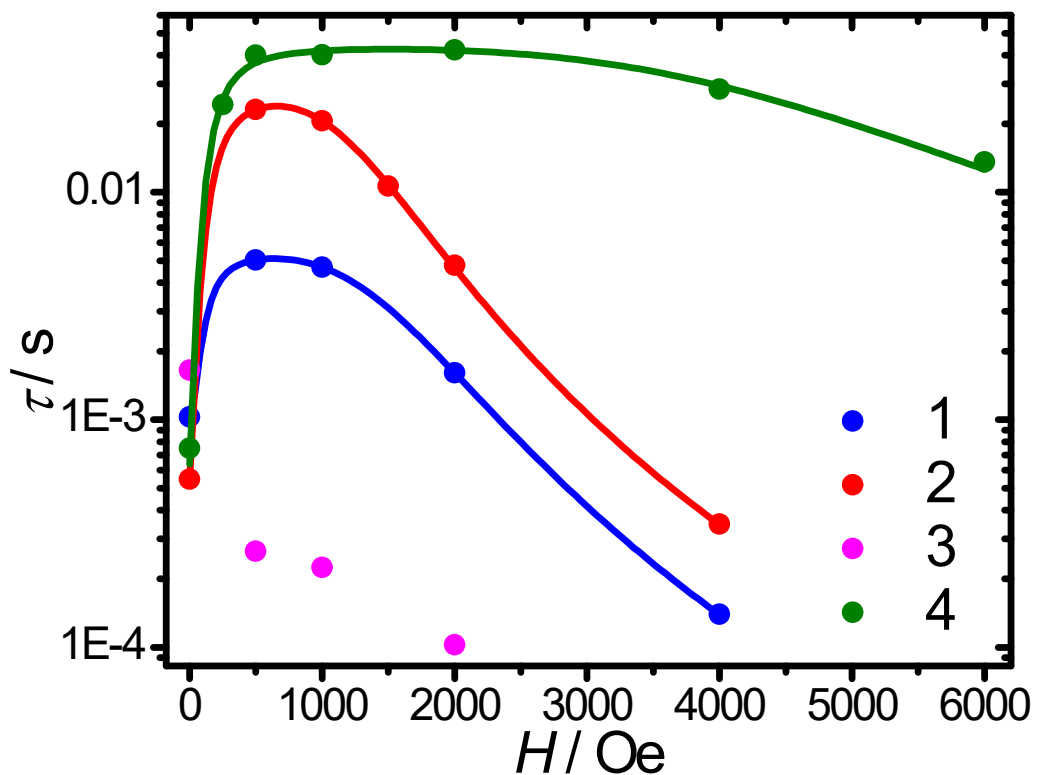


Figure S7: Field dependence of the relaxation time at 2 K (1-3) and 5 K (4). The solid line represents the fit with Eq. 2.

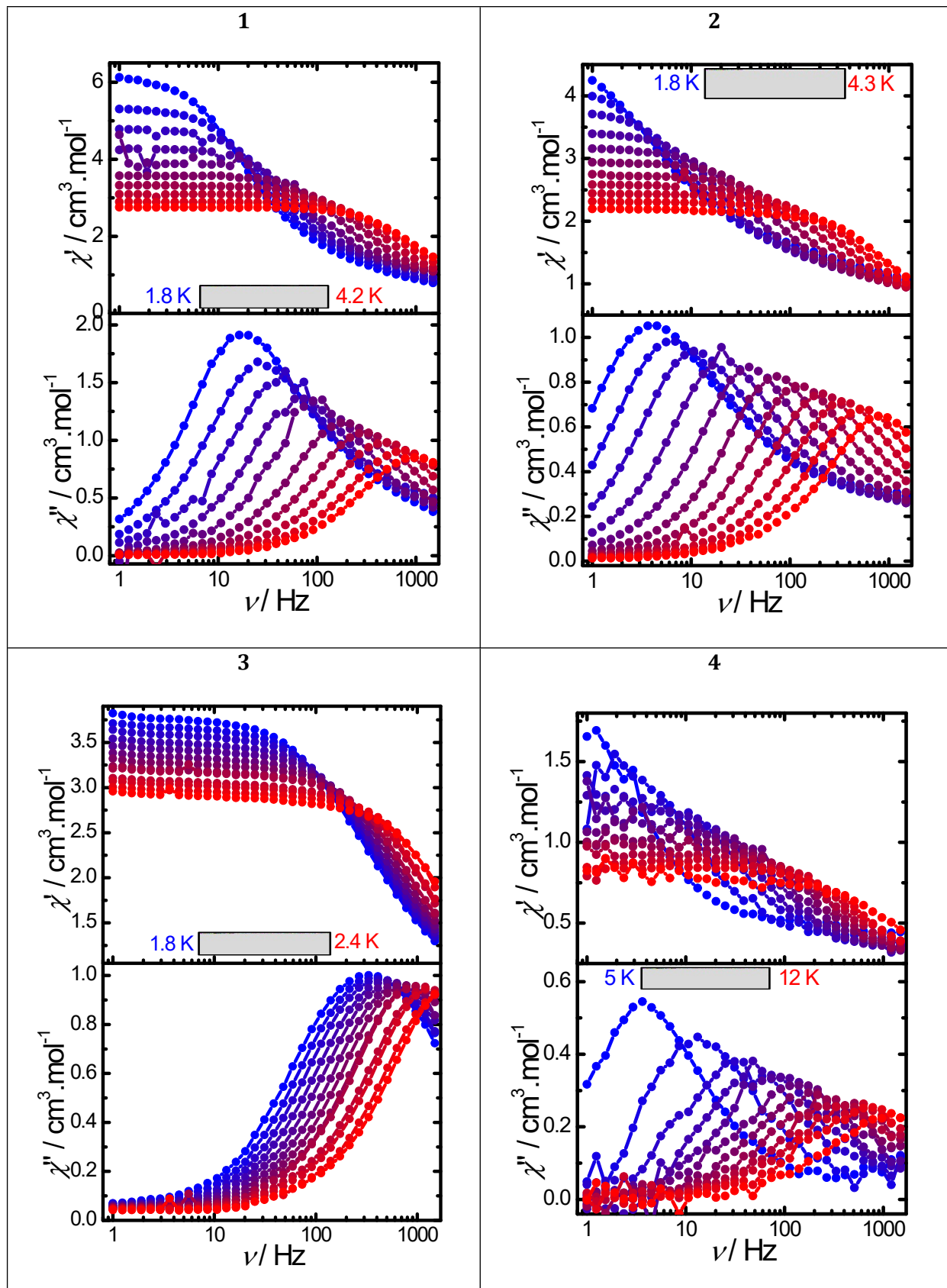


Figure S8: Frequency dependence of χ' and χ'' for different temperatures performed under a 500 (1-3) or 1000 (4) Oe dc field.

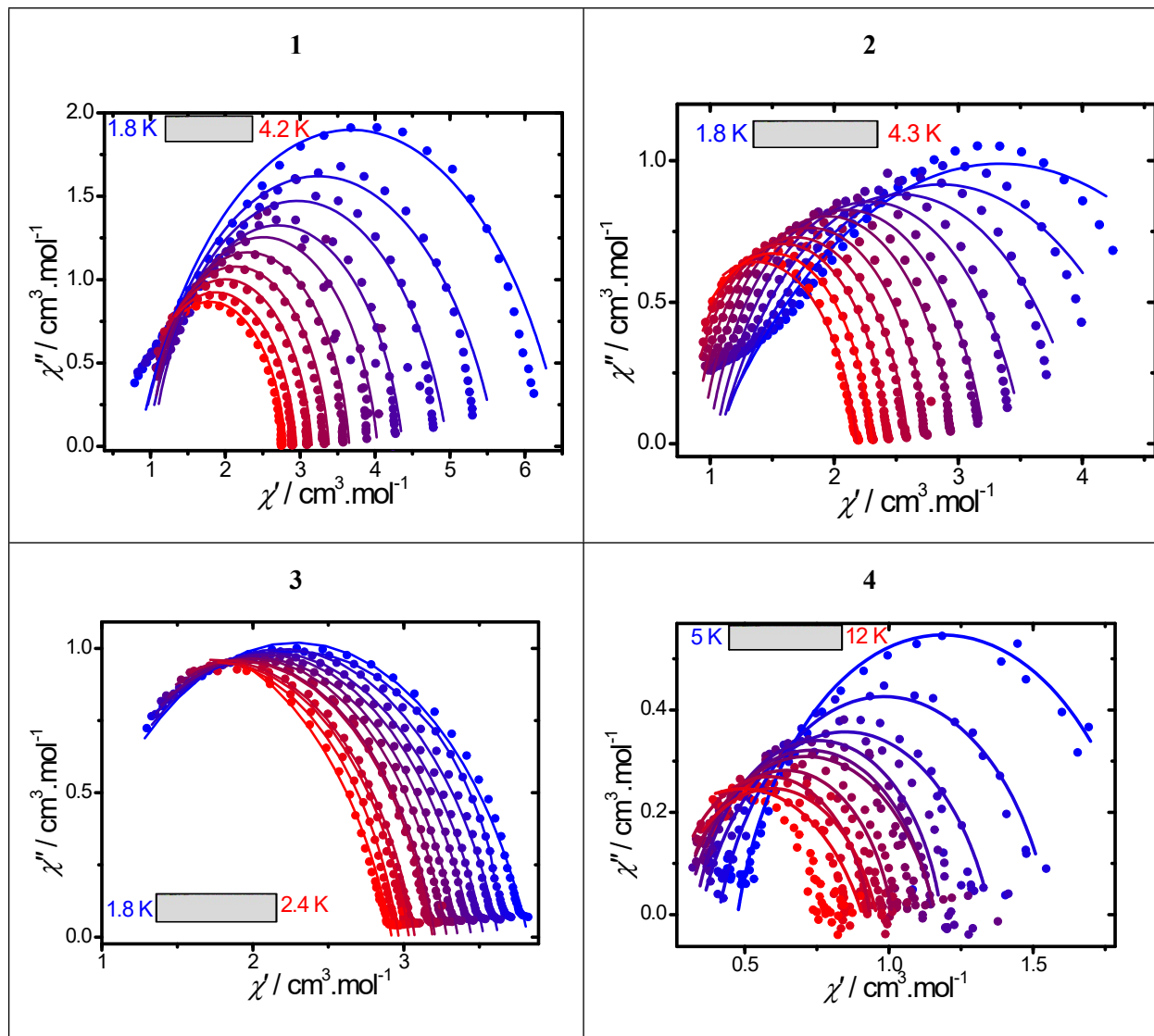


Figure S9: Cole-Cole (Argand) plots obtained using the ac susceptibility data for **1-3** (500 Oe) and **4** (1000 Oe). The solid lines correspond to the best fit obtained with a generalized Debye model.

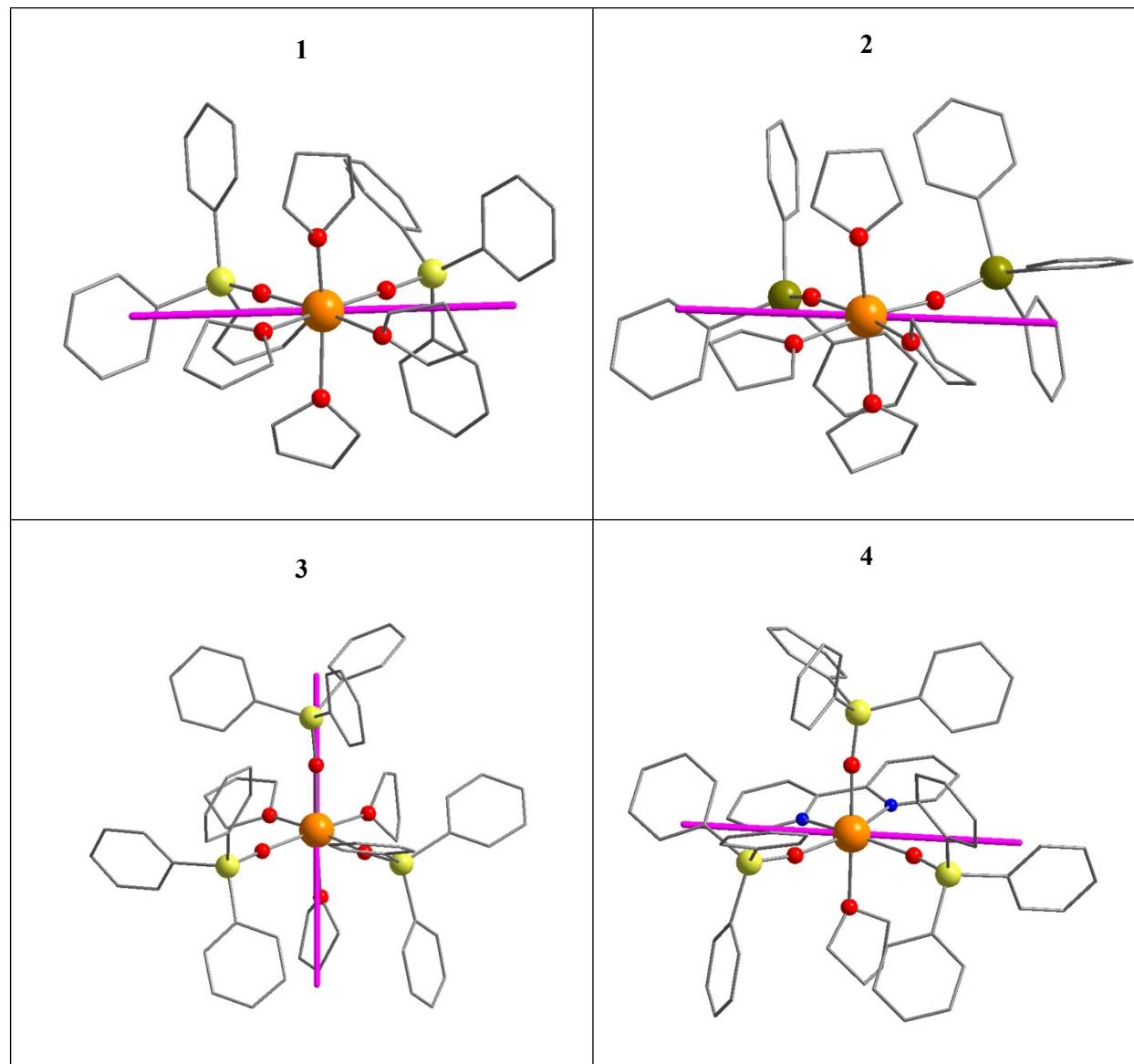


Figure S10: Anisotropic axes (purple) obtained from the MAGELLAN package.¹

Table S1: Crystal data, data collection and structure refinement details for **1**, **2**, **3**, **4**.

	1	2	3	4
Formula	$2\text{C}_{52}\text{H}_{62}\text{DyO}_6\text{Si}_2$, $2\text{C}_{24}\text{H}_{20}\text{B}$, $2\text{C}_4\text{H}_8\text{O}, \frac{1}{2}\text{C}_6\text{H}_{14}$	$\text{C}_{52}\text{H}_{62}\text{DyO}_6\text{Sn}_2$, $\text{C}_{24}\text{H}_{20}\text{B}, \text{C}_6\text{H}_{14}$	$\text{C}_{66}\text{H}_{69}\text{DyO}_6\text{Si}_3$, $\text{C}_4\text{H}_8\text{O}$	$\text{C}_{68}\text{H}_{61}\text{DyN}_2\text{O}_4$ $\text{Si}_3, \text{C}_4\text{H}_8\text{O}$
<i>M</i>	2825.06	1588.27	1277.08	1289.06
<i>T</i> , K	120	100	120	100
Crystal system	Monoclinic	Triclinic	Monoclinic	Monoclinic
Space group	<i>C</i> 2/ <i>c</i>	<i>P</i> - <i>I</i>	<i>P</i> 2 ₁	<i>P</i> 2 ₁
<i>Z</i> (<i>Z'</i>)	8 (1)	2 (1)	2 (1)	2 (1)
<i>a</i> , Å	46.8542(19)	14.2076(6)	14.334(2)	14.2745(4)
<i>b</i> , Å	18.1479(8)	14.4956(6)	16.468(2)	16.2901(5)
<i>c</i> , Å	18.2239(8)	20.1298(8)	14.540(2)	15.0762(4)
α , deg	90	75.221(2)	90	90
β , deg	112.5840(10)	83.003(2)	113.635(3)	115.8060(10)
γ , deg	90	64.8030(10)	90	90
<i>V</i> , Å ³	14307.6(11)	3626.7(3)	3144.3(8)	3156.10(16)
<i>d</i> _{calcd} , g·cm ⁻³	1.312	1.454	1.349	1.356
μ , mm ⁻¹	1.132	1.755	12.98	1.293
<i>F</i> ₀₀₀	5884	1614	1322	1326
2 <i>θ</i> _{max} , deg	50.00	57.57	52	60.22
Number of measured refl.	54365	51646	41242	52387
Number of independent refl. (<i>R</i> _{int})	12598 (0.0870)	18780 (0.0529)	12339 (0.1365)	18482 (0.0392)
Observed refl. [<i>I</i> > 2σ(<i>I</i>)]	8557	13051	9051	15818
Parameters	875	899	741	796
<i>R</i> ₁ [<i>F</i> ² > 2σ(<i>F</i> ²)]	0.0598	0.0452	0.0564	0.0349
<i>wR</i> ₂ (all data)	0.1570	0.0901	0.1104	0.0572
<i>S</i> (<i>F</i> ²)	1.016	1.040	0.996	1.031
Residual density (<i>d</i> _{max} / <i>d</i> _{min}), e·Å ⁻³	2.26 / -2.03	2.17 / -1.60	1.29/-1.10	0.66 / -0.54

Table S2: SHAPE analysis for 1-4.

	HP	PPY	OC	TPR	JPPY
1	31.923	27.382	0.461	14.634	30.968
2	32.907	27.334	0.429	15.136	31.036
3	32.708	29.268	0.414	16.110	32.752
4	31.347	23.384	1.907	10.947	27.345

HP: Hexagon

PPY: Pentagonal Pyramid

OC: Octahedron

TPR: Trigonal Prism

JPPY: Johnson Pentagonal Pyramid

Table S3: Selected bond lengths (\AA) and angles (deg) for **1-4**.

1	
Dy(1)-O(1)	2.093(5)
Dy(1)-O(2)	2.108(5)
Dy(1)-O(3)	2.357(7)
Dy(1)-O(4)	2.405(5)
Dy(1)-O(5)	2.410(5)
Dy(1)-O(6)	2.331(5)
O(1)-Dy(1)-O(2)	102.6(2)
2	
Dy(1)-O(1)	2.068(3)
Dy(1)-O(3)	2.358(3)
Dy(1)-O(2)	2.068(3)
Dy(1)-O(4)	2.473(3)
Dy(1)-O(5)	2.430(3)
Dy(1)-O(6)	2.366(3)
O(2)-Dy(1)-O(1)	105.2(2)
3	
Dy(1)-O(1)	2.118(8)
Dy(1)-O(2)	2.136(8)
Dy(1)-O(3)	2.132(8)
Dy(1)-O(4)	2.478(8)
Dy(1)-O(5)	2.448(8)
Dy(1)-O(6)	2.423(8)
O(1)-Dy(1)-O(2)	102.0(3)
O(1)-Dy(1)-O(3)	101.8(3)
O(2)-Dy(1)-O(3)	101.2(3)
4	
Dy(1)-O(1)	2.123(2)
Dy(1)-O(2)	2.135(3)
Dy(1)-O(3)	2.135(2)
Dy(1)-O(4)	2.402(8)
Dy(1)-N(1)	2.518(3)
Dy(1)-N(2)	2.543(3)
O(1)-Dy(1)-O(2)	96.9(2)
O(1)-Dy(1)-O(3)	99.4(2)
O(2)-Dy(1)-O(3)	111.7(2)
N(1)-Dy(1)-N(2)	63.5(2)

Table S4: Fitting of the Cole-Cole plots with a generalized Debye model under a 0 Oe dc field for **4**.

T (K)	χ_S (cm ³ . mol ⁻¹)	χ_T (cm ³ . mol ⁻¹)	α
1.8	1.18436	4.92321	0.27607
2.61977	0.88795	3.44602	0.27619
3.4398	0.68705	2.7122	0.30912
4.25836	0.56742	2.18912	0.30963
5.07962	0.55174	1.80843	0.23543
5.89962	0.46386	1.55925	0.23382
6.71949	0.47892	1.37382	0.15486
7.53918	0.40634	1.21703	0.14317
8.35943	0.37068	1.09015	0.11905
9.17917	0.32283	1.01084	0.11746
9.99874	0.25093	0.95505	0.16096

Table S5: Fit parameters of the field dependence of the relaxation time at 30 K for **1**, **2** and **4**.

<i>Compound</i>	D (s ⁻¹ K ⁻¹ Oe ⁻⁴)	B_1 (s ⁻¹)	B_2 (Oe ⁻²)	K
1 (2 K)	1.37×10^{-11}	791.1	2.2×10^{-4}	182.4
2 (2 K)	5.59×10^{-11}	1786.5	1.0×10^{-3}	35.7
4 (5 K)	8.71×10^{-15}	1544.2	1.5×10^{-3}	22.8

Table S6: Fitting of the Cole-Cole plots with a generalized Debye model under a 500 Oe dc field for **1**.

T (K)	χ_S (cm ³ . mol ⁻¹)	χ_T (cm ³ . mol ⁻¹)	α
1.79965	0.8376	6.52562	0.25055
2.07507	0.85156	5.62576	0.2406
2.35002	0.9557	4.97048	0.19423
2.62481	1.03054	4.37047	0.14566
2.89974	0.98583	4.03259	0.12286
3.17458	0.95627	3.65514	0.09389
3.4497	0.8889	3.38252	0.09188
3.72527	0.84148	3.15429	0.09081
3.99958	0.79866	2.94799	0.09585
4.19853	0.78599	2.80487	0.09651

Table S7: Fitting of the Cole-Cole plots with a generalized Debye model under a 500 Oe dc field for 2.

T (K)	χ_s (cm ³ . mol ⁻¹)	χ_T (cm ³ . mol ⁻¹)	α
1.80218	1.00325	5.6707	0.48934
2.04996	1.05139	4.66984	0.40316
2.30018	1.06192	4.02239	0.31654
2.5498	1.03558	3.53514	0.23601
2.79963	0.98364	3.21668	0.18857
3.04951	0.9309	2.96962	0.14965
3.29967	0.8645	2.75051	0.13397
3.54972	0.7954	2.59521	0.13293
3.79977	0.75656	2.43587	0.10981
4.04886	0.698	2.30415	0.11186
4.29848	0.57322	2.18138	0.14158

Table S8: Fitting of the Cole-Cole plots with a generalized Debye model under a 500 Oe dc field for 3.

T (K)	χ_s (cm ³ . mol ⁻¹)	χ_T (cm ³ . mol ⁻¹)	α
1.79968	0.74388	3.8234	0.25486
1.84993	0.73539	3.71751	0.24394
1.8997	0.75153	3.6271	0.22737
1.94989	0.71801	3.53032	0.22192
1.99986	0.71799	3.44788	0.20788
2.04986	0.7162	3.35793	0.19516
2.0998	0.67638	3.2847	0.18849
2.14981	0.61073	3.20706	0.1888
2.2498	0.46786	3.07257	0.19034
2.29994	0.51861	3.03322	0.17492

Table S9: Fitting of the Cole-Cole plots with a generalized Debye model under a 1000 Oe dc field for 4.

T (K)	χ_s (cm ³ . mol ⁻¹)	χ_T (cm ³ . mol ⁻¹)	α
4.99973	0.475	1.9	0.165
5.99929	0.409	1.56	0.188
6.99907	0.346	1.35	0.214
7.499	0.328	1.18	0.143
7.99948	0.297	1.16	0.182
8.49883	0.266	1.16	0.23
8.99932	0.273	1.01	0.169
9.49928	0.237	0.933	0.16
9.99876	0.232	0.957	0.239
10.49756	2.15E-14	0.967	0.419
10.99589	0.0761	0.908	0.32

References

- 1 N. F. Chilton, D. Collison, E. J. L. McInnes, R. E. P. Winpenny and A. Soncini, *Nat. Commun.*, 2013, **4**, 2551.